Biogeosciences
Discussions
Open Access
EGU

# Do bacterial viruses affect the framboid-like mineral formation?

Paweł Działak[1], Marcin D. Syczewski[2], Kamil Kornaus[3], Mirosław Słowakiewicz[2], Łukasz Zych[3], Andrzej Borkowski[1]

[1]Faculty of Geology, Geophysics and Environmental Protection, AGH University of Science and Technology, Al. Mickiewicza 30, 30-059 Krakow, Poland.
[2]Faculty of Geology, University of Warsaw, ul. Żwirki i Wigury 93, 02-089 Warsaw, Poland.
[3]Faculty of Materials Science and Ceramics, AGH University of Science and Technology, Al. Mickiewicza 30, 30-059 Krakow, Poland.

*Correspondence to*: Paweł Działak (dzialak@agh.edu.pl)

**Abstract.** Framboidal pyrite has been a matter of interest of many studies due to its abundance in a wide range of environments, and as a marker of redox conditions. However, the clear origin of framboidal pyrite remains unresolved. The paper discusses the possible role of bacteriophages (bacterial viruses) in the precipitation of sulphide minerals (FeS and CuS) and their impact on the formation of framboid-like structures. Here, two bacteriophages (Enterobacteria phage P1 and Pseudomonas phage Φ6), which differ significantly in the shape and physicochemical properties, were used. Our observations suggest that viruses can attract ions from the solution and thus change the electrochemical properties of precipitated minerals. Moreover, we showed that bacteriophages P1 can lead to the formation of finer mineral particles of FeS and CuS, whereas the framboid-like structures were found only in experiments with precipitation of FeS. However, Pseudomonas phage Φ6 did not cause formation of similar structures probably due to the presence of lipid envelope. Hence, it is assumed that Enterobacteria phage P1 can promote the formation of the FeS-based framboid-like structures. The proposed four-step conceptualized mechanism of the framboidal-like structure synthesis via viruses is as follows: (i) attraction of ions by capsids, (ii) bacteriophages behave like nuclei for mineral crystallisation, (iii) destabilisation of the colloid ($\zeta$-potential $\sim 0$), (iv) formation of fine agglomerates.

## 1 Introduction

Currently, the microorganisms are known to play a pivotal role during the formation and precipitation of mineral phases. Bacterial and archaeal activity can lead to a change in physicochemical conditions in the various environments, under both aerobic and anoxic conditions. For example, biochemical activity can lead to the formation of various biominerals (Lowenstam, 1981) and mechanisms responsible for their formation are termed biomineralization (Lowenstam and Weiner, 1989; Mann, 1988). Microbial activity can also strongly affect the sulphide oxidation process leading to the formation of acid mine drainage (Chen et al., 2016). On the other hand, sulphate-reducing bacteria can produce sulphides under anaerobic conditions (Muyzer and Stams, 2008) and this process was crucial in some circumstances in the formation of various metal ores. In certain processes, sulphide minerals can be shaped as framboid-like structures. The framboid is a commonly known

micromorphological feature of some sedimentary minerals, e.g., framboidal pyrite (Wilkin and Barnes, 1997) and framboidal magnetite(Hua and Buseck, 1998). The creation of framboidal pyrite or framboidal greige (a precursor of pyrite) can be linked (i) with reducing conditions in sediments where $H_2S$ is produced, and (ii) with euxinicc water where sulphides and no-

35 oxygen conditions coexist (Popa et al., 2004). Hence, the framboidal pyrite in some sediments is used as a marker of the redox conditions that occurred during sedimentation. However, it is not clear how the framboidal structure is created. Some experiments conducted under laboratory conditions showed that framboid-like pyrite can be synthesized abiotically (Ohfuji and Rickard, 2005). On the other hand, it was postulated that these structures can be formed through microbial activity (Popa et al., 2004). It should be emphasized that one does not exclude the other. However, an additional possible factor, which

40 should be discussed is involvement of bacteriophages (bacterial viruses). Many viruses have a symmetric, crystal-like structure that can be analysed with X-ray diffractometry. Most of them have icosahedral capsid (virus head) without an outer lipid membrane. Interestingly, bacterial viruses have not been studied so far as crystallization factors in sulphide environments, especially their involvement in the formation of framboid-like structures. Only a few studies have been conducted so far in relation to modern siliceous (Daughney et al., 2004; Laidler and Stedman, 2010; Peng et al., 2013), iron-

45 rich (Kyle et al., 2008; Orange et al., 2011), carbonate (Pacton et al., 2015; Słowakiewicz et al., 2021; Perri et al., 2022), and microbial mat (De Wit et al., 2015; Perri et al., 2018; Pennafirme et al., 2019; Pacton et al., 2014; Carreira et al., 2015) environments. In addition, the abundance of viral particles in water or sediments can exceed the number by bacteria of orders of magnitude (Fuhrman, 1999; Steward et al., 1996). The number of bacteriophages is estimated to be $10^4$ to $10^8$ per mL in aquatic environments (Wittebole et al., 2014). Viruses studied here have different shapes and diameters. *Pseudomonas phage*

50 Φ6 has an icosahedral shape (60 nm in diameter) and a lipid envelope (Vidaver et al., 1973), while *Enterobacteria phage* P1 has an icosahedral shape (75 nm in diameter) with a long tail (220 nm in length) (Fermin et al., 2018). Considering the physicochemical properties of the bacteriophages it can be assumed that the mineral precipitation can be affected by viral capsids. The dimension of capsids is very small; in bacteriophages, it is about 50 – 200 nm. Several studies showed that viruses can be used as a modifying factor that affects the precipitation of various nanomaterials (Ivanovska et al., 2004; Nam

55 et al., 2004; Slocik et al., 2005). In laboratory experiments, bacteriophages were also shown to likely influence vaterite formation – a metastable form of calcium carbonate (Słowakiewicz et al., 2021). That viruses can play an important role during the sedimentation processes has not been widely tackled so far. Therefore, is it possible that viruses can induce or influence the formation of framboid-like structures during the mineral precipitation? Considering the crystal-like structures of capsids and their dimensions, as well as various net-surface charges, this question seems to be well-founded. Importantly,

60 in this respect the role of viruses in the formation of framboids has not been studied so far. Therefore, in our paper, we demonstrate experiments that test the hypothesis that framboid-like structures can be created during mineral precipitation in the presence of bacterial viruses. For obvious reasons, we focussed on sulphide minerals, but we did not assume that these structures cannot be formed by precipitation of other mineral phases. The formation of sulphide framboids in the presence of viruses can be extremely important for the correct interpretation of the presence of such structures in sediments and aquatic

65 systems with the developed euxinic zone.

## 2 Materials and Methods

### 2.1 Preparation of bacteriophages and experimental setup

The overall scheme of the experiments is presented in Figure 1.

### 2.1.1 Preparation of bacteriophages

*Enterobacteria phage* P1 and *Pseudomonas phage* Φ6 were obtained from the Leibniz Institute DSMZ-German Collection of Microorganisms and Cell Cultures. Three media were prepared: bottom agar – tryptic soy broth (TSB) containing 1.5 % agar; top agar - TSB containing 0.75 % agar; and liquid TSB without agar. The media were sterilised at 121°C for 30 min and cooled down to 50°C. Bottom agar was poured onto the Petri dishes, and plates were dried to remove the condensed vapour on the surface of the solid medium. It is crucial to dry plates before pouring the top agar, e.g., in a laminar chamber. Otherwise, the top agar layer will not adhere to the bottom agar. Sterile 1M $MgSO_4$ solution was added to the cooled liquid TSB and the final concentration was set at 5 mM. To a 15-mL tube with 0.1 mL of diluted bacteriophage solution, 1 mL of liquid TSB containing 5 mM $MgSO_4$ and 0.1mL of an overnight (18 h) liquid bacterial culture was added ($OD_{550}$ ranges for *Escherichia coli* and *Pseudomonas syringe* were 0.7-0.9 and 0.4-0.5, respectively*). Cooled top agar (4 mL) containing 5 mM $MgSO_4$ was added to the bacterial solution. The tube was gently mixed, and the solution was immediately poured onto a bottom agar plate. Solidified plates were incubated for 24 h at 37°C and 48 h at 25°C for the *E. coli* and *P. syringe,* respectively. The latter cannot be overheated because high temperature prevents their growth.

### 2.1.2 Purification of bacteriophages

The top agar was scraped using a glass rod and transferred to a 50 mL polypropylene tube. A 20 mL of sterile bacteriophphage buffer ($MgCl_2$ 20 mM and Tris-HCl 20 mM) was added and the mixture was thoroughly mixed using vortex. Optionally, 3 mL of chloroform can be added to the *Enterobacteria phage* P1 culture to facilitate the removal of bacterial debris. Importantly, chloroform destroys the lipid envelope of *Pseudomonas phage* Φ6, therefore the solvent cannot be added. The mixture was centrifuged at 4400×g for 5 min to remove agar.

The supernatant was transferred to 2 mL polypropylene tubes. The tubes were firstly spined at 13000×g for 5 min to remove the bacterial debris. The supernatant was transferred to 2 mL tubes. The tubes were centrifuged at 24000×g for 45 min at 5°C. The supernatant was discarded and the tubes with pellet were centrifuged to remove the remaining liquid. Viral pellets were visible with a naked eye.

1 mL of a sterile 0.9 % NaCl solution was added to the first tube and the pellet was resuspended. The whole solution was transferred to the next tube and used to resuspend the pellet. This step was repeated until all pellets in the tubes were resuspended. The solution was placed in a 15-mL polypropylene tube and 14 mL of sterile 0.9 % NaCl was added. The solution can be stored in the fridge at 5°C for up to one month.

### 2.1.3 Quality control

Viral solution (0.1 mL) was mixed with 10 µL of the previously diluted (10000×) Sybr®Gold dye. The solution was placed on a microscopic slide and examined using an epifluorescence microscope with the blue filter (DM500 filter with a band-pass 460-490 nm excitation filter). The count of bacteriophage particles was estimated using plate techniques with serial dilution of bacteriophages suspension obtained after purification step. Additionally, the UV-related empirical formula was used to quickly assess the density of bacteriophage suspension:

$$\frac{virions}{mL} = \frac{(A_{269} - A_{320}) \cdot 6 \cdot 10^{16}}{number\ of\ bases/virion} \text{ (Day and Wiseman, 1978)}$$

In all experiments, the density of bacteriophages suspension was normalised to $10^{10}$ mL$^{-1}$.

### 2.1.4 Precipitation experiments

Solutions of $FeSO_4$, $CuSO_4$, and $Na_2S$ (0.2 M) were prepared. A beaker with 10 mL of $FeSO_4$ or $CuSO_4$ solution was thoroughly mixed on a magnetic stirrer (stirring condition) or without stirring. Importantly, iron sulphide precipitation was carried out under an oxygen-free atmosphere (chamber Secador Techni-Dome 360). The bacteriophage solution (1 mL) and the subsequent $Na_2S$ solution were poured according to two variants: (i) 2 to 20 µL of $Na_2S$ for ζ-potential and size distribution measurements; (ii) 5 mL of $Na_2S$ (in 0.5 mL portions) for SEM and XRD analysis. For SEM and XRD analyses, the obtained precipitates were centrifuged, the supernatant was discarded, and the pellet was washed in pure water. Eventually, the pellet was resuspended in 10 mL of analytical grade acetone (Fig. 1).

### 2.2 ζ-potential measurements and Z-average size distribution

ζ-potential and Z-average size distribution measurements were obtained using a Zetasizer Nano-ZS (Malvern).

### 2.2.1 Isoelectric point of bacteriophages

To find the isoelectric point of bacteriophages, a series of measurements was carried out in a phosphate buffer with pH ranging from 4.5 to 8. The bacteriophage solution (1 mL) was mixed with 14 mL of buffer at the fixed pH (4.5; 5.6; 6.2; 7.0; 7.5) and then placed in a measurement cell.

### 2.2.2 Ion attraction by bacteriophages

The measurements were carried out to measure the possibility of viral capsids to attract ions present in the solution. The solution of bacteriophages (1 mL) was mixed with 5 mL of $FeSO_4$ (0.2 M), $CuSO_4$ (0.2 M), or $Na_2S$ (0.2 M). Samples were incubated for 3 to 5 min and then measured.

### 2.2.3 Measurements of sulphide precipitates

$\zeta$-potential measurements were performed to check possible changes in $\zeta$-potential of precipitated minerals in the presence of
135 viruses. The reaction mixture was placed in a measurement cell after the precipitation as described in Section 2.1.4 in variant
(i). Additionally, the Z-average size distribution measurements were conducted. However, due to strong agglomeration, the
obtained results may exceed the measurement range of device.

### 2.3 XRD

140 The X-ray diffraction analysis was performed with a Malvern Panalytical X'Pert PRO MPD (Malvern Panalytical, Malvern,
UK) diffractometer. Registration was carried out with a CoK$\alpha$ lamp at 40 kV and 30 mA in the range of 4–84$^O$ 2$\theta$ with a step
of 0.0260$^O$ 2$\theta$. The results were analysed using X'Pert Plus HighScore software with access to the Crystallography Open
Database.

### 2.4 Electron microscopy

145
Microscopic analyses were conducted using a Carl Zeiss AURIGA (Carl Zeiss Microscopy GmbH) field emission scanning
electron microscope (SEM) coupled with two energy-dispersive spectrometers XFlash 6|30 (Bruker Nano GmbH).
Crystallite samples were placed on the glass slide and coated with 20 nm layer of carbon by a vacuum coater (Quorum 150T
ES). Analysis was done with a 20 kV acceleration voltage, a 120 µm aperture, and the working distance at approximately 10
150 mm. The bacteriophage characterisation was conducted using a scanning transmission electron detector on the same
microscope. A drop of purified bacteriophages was applied on a TEM mesh covered with a carbon foil with a thickness of 3
nm. Next, they were contrasted with 1% solution of uranyl nitrate for 2 min and subsequently dried out. Finally, they were
coated with 8 nm of chromium layer by vacuum coater. Analysis was done with bright field mode at 30 kV acceleration
voltage, a 120-µm aperture, and the working distance at approximately 10 mm.

155

### 3 Results

The procedure of obtaining pure bacteriophage suspensions was highly efficient. The obtained bacteriophages were clearly
visible after Sybr®Gold staining due to the agglomeration occurring especially when the density of bacteriophages
suspension exceeded $10^{10}$ mL$^{-1}$. Furthermore, the obtained suspension was free from bacterial debris, as can be seen in the
160 epifluorescence microscopic and SEM images (Fig. 2). The yield of bacteriophages was in the range of $1\times10^8$ to $1\times10^{11}$
bacteriophages mL$^{-1}$ and before the next experiments bacteriophage suspensions were normalised to $10^{10}$ mL$^{-1}$.

### 3.1 $\zeta$-potential measurements of bacteriophages

The measurements have revealed that $\zeta$-potential is different for both bacteriophages and is pH-dependent (Fig. 3a). Under
165 the tested pH, it has not been possible to obtain the $\zeta$-potential value of zero and thus determine the isoelectric point. For the

pH range of 5.6 to 7.5, the ζ-potential for both bacteriophages were considerably stable, ranging from -5 to -15 mV. At pH 4.5, the ζ-potential of P1 reached -27 mV, while for Φ6 the potential reached -2 mV.

### 3.2 ζ-potential measurements and Z-average size distribution of precipitates

170 Measurements of FeS precipitates (Fig. 3b) have shown that there is a difference between the sample without viruses and with both types of bacteriophages. Data analysis has shown that the differences among samples were statistically significant (**). It should be noted that ζ-potential in the attempt of CuS (Fig. 3b) with the bacteriophage P1 has changed to positive values (+1mV). The conductivity was not significantly different in all samples and ranged from 15 to 16 mS/cm (Fig. 3b). The conductivity was measured for control purposes to check whether the ionic strength was similar in all samples.

175 ζ-potential of both bacteriophages at pH 7 in phosphate buffer was below -10 mV (Fig. 3a). In case of both bacteriophage suspensions in 0.9 % NaCl solution, ζ-potential was still negative but slightly lower (Fig. 3c). For bacteriophage P1 addition of $FeSO_4$ and $CuSO_4$ caused a slight, but significant change (-3.3 and -3.7 mV respectively). However, addition of $Na_2S$ increased the potential significantly (-15.8 mV). In case of bacteriophage Φ6, ζ-potential was -3.1 mV. Addition of $FeSO_4$, $CuSO_4$ caused only an insignificant change (-0.9 and -1.22 mV, respectively). However, addition of $Na_2S$ increased the

180 potential significantly (+11.9 mV).

The measurement of Z-average size distribution (Fig. 3d) has revealed that addition of bacteriophages to the reaction mixture significantly changed the size of precipitated FeS and CuS particles. There has been an increase of 275% (2000 nm - 5500 nm) and 405% (2000 nm - 8100 nm) for FeS+P1 and FeS+Φ6 respectively. For CuS+P1 and CuS+Φ6, addition of bacteriophages caused the formation of smaller particles. There has been about 70% decrease in size of precipitates (5900 to

185 4500 nm and 5900 to 4000 nm respectively).

### 3.3 XRD

The X-ray diffraction results are presented in Figure 4. Phase composition of samples did not differ significantly. The strongest signals derived from mineral phases resulted from oxidation of samples during the grinding and preparation of

190 samples for XRD analysis. In copper sulphide synthesis, traces of covellite were found. However, its identification was hampered by oxidation products, other synthesis products, and residual substrates used in the synthesis. The XRD results confirmed the presence of kröhnkite, chalcanthite, and natrochalcite. Traces of pyrite and troilite were confirmed in the synthesis of iron sulphides. Like in copper sulphides, the analysis of iron sulphides did not differ significantly probably due to the oxidation of samples. The results additionally proved the presence of mohrite, butlerite, and jarosite.

195

### 3.4 Morphology of FeS and CuS precipitates

In order to check whether the observed mineral phases were ferrous and copper sulphides, the EDS spectra were measured for every observed phase. The EDS spectrum should not contain significant signals indicating oxygen and sodium in the sample. Such elements could indicate the impurities from reagents or products after reaction, and the observed crystals

200  probably were sulphates. In Figure 5 samples of EDS spectra of mineral phases observed under SEM are presented. Spectra 1 and 2 revealed distinct signals from iron and sulphur. Neither oxygen nor sodium in significant quantity were noted. Such spectra suggest that the observed phases were ferrous sulphides. If these spectra revealed strong signals of sodium and/or oxygen (e.g. spectrum 3), the observed mineral phases were not further analysed. In case of copper sulphide, the same approach was used. Spectra 4 and 5 contain strong signals of copper and sulphur. Oxygen and sodium were hardly detected.

205  Hence, it can be assumed that the observed phases were copper sulphides. Spectrum 6 revealed strong signals indicating sodium and probably mineral phases contained sulphates.

The obtained precipitates of FeS with and without P1 bacteriophage under both stirring and without stirring conditions were examined under SEM to analyse the morphology and dimension of the single and agglomerated/aggregated particles (Fig. 6). The stirring conditions during our experiment caused the precipitation of quite massive structures that consisted of visible

210  smaller particles (Fig. 6 a-d). Experiments with bacteriophages gave similar structures. However, much smaller particles were noted in comparison to control experiments (Fig. 6 f,g). Furthermore, very small particles with dimensions close to 200 – 300 nm were found in great numbers (Fig. 6 h), while similar particles were not observed in control experiments (the smallest particles were approximately 0.8 – 1 µm; Fig. 6d). It should be emphasized, that the framboid-like structures were not found in both experiments conducted under stirring conditions.

215  It would seem that a similar situation was observed in experiments under non-stirring conditions (Fig. 6, control: i–l; with bacteriophages: m–p). In experiments with bacteriophages, much smaller particles building larger agglomerates/aggregates were noted in comparison to the control sample. Very small particles were also observed (Fig. 6p), like in experiments under stirring conditions (Fig. 6h). However, the precipitated mineral phases with bacteriophages under non-stirring conditions revealed spheroidal structures that were composed of finer particles (Fig. 6 m-o). These spheroidal structures resemble

220  framboid-like structures and were not observed in control experiments. The diameter of these structures was about 1 µm to more than 10 µm. Analogous experiments were conducted with $\Phi 6$ bacteriophages (Fig. 7) to check whether the bacteriophage capsids enveloped by lipid membrane can cause similar effects as in P1 bacteriophages. It should be noted that $\Phi 6$ phage caused the overrepresentation of smaller mineral particles similar to P1 phage. However, neither stirring nor non-stirring conditions caused the precipitation of framboid-like structures. Only the potentially spheroidal structures could be

225  seen (Fig. 7c), but these structures were not as clear as in experiments with P1 phage.

It was also interesting to check whether the framboid-like structures may appear in presence of bacteriophages in case of non-ferrous sulphides. The copper sulphide can be precipitated much more easily in comparison to ferrous compounds, especially due to its higher stability under oxygen atmosphere. The experiments with copper compounds and P1 bacteriophages were conducted under stirring and non-stirring conditions, and the obtained mineral phases were examined

230  under SEM (Fig. 8). The obtained results indicate that the presence of bacteriophages in the reaction mixture can strongly induce the creation of agglomerates/aggregates that were built of smaller particles in relation to control experiments without bacteriophages. Similar observations were noted in non-stirring FeS experiments, but here it was especially visible in experiments under stirring conditions. The control precipitation created 'massive' agglomerates formed by large particles

(Fig. 8 a-d). In contrast, in experiments with bacteriophages, the precipitates consisted of fine particles (Fig. 8 e-h). This

235 difference was even clearly visible with a naked eye. CuS precipitates in suspension after precipitation in the presence of P1 bacteriophages had a fine, sand-like texture, while CuS precipitates without bacteriophages formed a more compact mass. It should be noted that the framboid-like structures were not observed in any CuS experiments.

**4 Discussion**

240 Viruses are at the border of the biotic and abiotic worlds. They do not carry any biological processes outside living cells. However, similar to other biological structures, they contain several proteins with different electrochemical properties. Thus, based on the DLVO theory (Derjaguin, Landau, Vervey, and Overbeek theory), it was assumed that viruses can behave as nuclei attracting ions from the solution and thus alter local physicochemical properties.

Daughney et al. demonstrated that virial capsids can attract iron ions and act as nuclei for the growth of iron-oxide particles

245 (Daughney et al., 2004). Our $\zeta$-potential measurements of viruses agree with the data provided by Daughney et al. Further, the $\zeta$-potential measurements in our study reveal that viruses have a pH dependent negative charge. The charge is stable at neutral pH. However, compared to the work of Daughney et al., here we used different types of bacteriophages (P1 and $\Phi6$) and different solutions (phosphate buffer), whereas Daughney et al. used PWH3a-P1 and 0.5M $NaNO_3$, respectively. Our assumptions further prove the hypothesis presented by Daughney et al. that viruses attract ions. $\zeta$-potential of capsids with

250 the $CuSO_4$ and $FeCl_2$ addition of solutions of $CuSO_4$ as well as $FeCl_2$ remained very similar to the control sample (pure viruses). However, the addition of $Na_2S$ drastically changed the $\zeta$-potential. It is assumed that P1 capsids (naked) tend to attract $S^{2-}$ ions, while $\Phi6$ capsids (enveloped) can attract $Na^+$. The lipid envelope of $\Phi6$ capsid includes a significant amount of phosphatidylglycerol, which contains negatively charged phosphate groups (Laurinavičius et al., 2004). Therefore, it can be concluded that these features caused $Na^+$ attraction. The P1 bacteriophage contains only proteins, which might contain

255 more positively charged groups, and thus attract $S^{2-}$ ions. Analysis of variance (ANOVA) showed that addition of every solution to P1 phage ($CuSO_4$, $FeCl_2$, $Na_2S$) caused a statistical change. For $\Phi6$ phage, a significant change was obtained only in the measurement with $Na_2S$.

Measurements of FeS and CuS precipitates in the presence of bacteriophages revealed that addition of viruses changed the $\zeta$-potential of mineral particles. There was an increase in the value of $\zeta$-potential in all samples. The charge was close to zero,

260 and thus it caused destabilisation of the colloid. The statistical significance test showed that the sample group FeS, FeS+$\Phi6$ and FeS+P1, as well as the group CuS, CuS+$\Phi6$, and CuS+P1, are statistically different. Statistical analysis confirmed our naked eye observations that the turbidity of the samples differed significantly. The precipitation experiment with bacteriophages has led to the formation of different structures, which formed visible agglomerates, whereas in control samples the phenomenon has not been observed.

265 The measured Z-average is the cumulative mean value of a set of particles measured by dynamic light scattering (DLS). The measurements showed that the size of FeS precipitates increased in samples with both types of bacteriophages, while the size of CuS precipitates behaved in the opposite way. This fact suggests that the average size of particles is bacteriophages-

dependent, but also depends on the precipitated sulphide. However, the measurement might be erroneous, due to the dynamic processes (aggregation or agglomeration) that might occur in the measurement cell.

270    The size of typical framboidal pyrite microcrystals ranges from 1 to 10 µm (Wilkin and Barnes, 1997) or from 0.1 to 20 µm (Scott et al., 2009), which exceeds the size of viruses. Furthermore, the single-framboidal pyrite microcrystal shape is described as icosahedral (Ohfuji and Akai, 2002) which is similar to the studied bacteriophages. This suggests that bacteriophages might affect sulphide precipitation due to their icosahedral capsid shape. However, there is no exact definition of framboidal pyrite, making the evaluation of these structures difficult. The diameter of framboidal pyrite can

275    vary, depending on the study: <10 µm, rarely >50 µm (Wilkin and Barnes, 1997), 30-80 to even 120 µm (in the Pleistocene sediments) (Ohfuji and Akai, 2002), 2 to 50 µm (Folk, 2005), 6 to 12.5 µm (Merinero et al., 2009), l-2 to 50-70 µm (Kortenski and Kostova, 1996). The origin of framboidal pyrite remains the subject of debate (Kalatha and Economou-Eliopoulos, 2015). Based on the available literature, it seems that framboidal pyrite may have a different origin depending on the environment. These structures have been found e.g., in sediments of euxinic basins (Wilkin et al., 1996); salt marsh

280    sediments (White et al., 1990); coal (early peat formation) (Wiese and Fyfe, 1986); or carbonate environments (Kobluk and Risk, 1977). Similar structures have also been found within bacterial cells (Donald and Southam, 1999)

An overview of the environments in which framboidal pyrite occurs, shows that it can be formed in many different backgrounds: oxic, dysoxic, or euxinic (Wilkin et al., 1997). Furthermore, framboidal pyrite has also been synthesized abiotically (Ohfuji and Rickard, 2005). Butler and Rickard used for such synthesis amorphous FeS, $H_2S$ and potassium

285    hydrogen phosphate/sodium dihydrogen phosphate buffer with an addition of Ti(III) citrate, at 60 to 100°C, and up to 45 days (Butler and Rickard, 2000). Wang and Morse used greigite and goethite and silica gel at room temperature and up to 24 months (Wang and Morse, 1996). Berner used $FeSO_4 \times 7H_2O$, $H_2S$ and $S^0$ at 65°C and 2 weeks (Berner, 1969). Farrand used $FeSO_4 \times 7H_2O$, $H_2S$, $CaCO_3$ and glycerine at room temperature and ~1 year (Farrand, 1970). Each of the previous examples required many reagents, or high temperatures, or a long time of the synthesis, which is entirely different from the conditions

290    presented in this work

Our synthesis of FeS-framboidal-like-structures was successful only in the trial with bacteriophages and without stirring. However, our framboid-like structures are very similar to "protoframboids" obtained by Wolthers (Wolthers, 2003; Wolthers et al., 2005) and Butler and Rickard (Butler and Rickard, 2000). The structures obtained by Wolthers are described as protoframboids formed on the euhedral-pyrite overgrowth. Such structures are about 1 µm in diameter and are described as

295    small and composed of poorly formed cubic pyrite microcrystals. Nonetheless, the experimental conditions of pyrite synthesis in our experiments were different. However, it seems likely that bacteriophages have led to the formation of similar structures (Fig. 9).

In stirred conditions, we assume that the fluid currents were created while stirring prevented framboid-like structures from forming. Nonetheless, viruses seem to be a strong factor that facilitate the formation of framboid-like structures. A

300    hypothetical pathway of the process is shown in Figure 10. After attracting ions present in the solution by viruses, a small amount of $S^{2-}$ ions added to the mixture caused precipitation of fine structures because of the net surface charge close to 0

mV. Under such conditions, phenomena such as aggregation or agglomeration may occur. In experiments without viruses, the charge is significantly more negative and thus, the colloid is stable (it does not precipitate immediately), so that no aggregation or agglomeration occurs at first. Subsequent addition of $S^{2-}$ ions releases a cascade process and the formation of

305 bigger structures.

There are several studies about formation of framboidal-like structures built of different minerals. Kerridge described magnetite (Kerridge, 1970), Nuhfer and Pavlovic reported greigite (Nuhfer and Pavlovic, 1979), and Taylor characterized magnesioferrite (Taylor, 1982). However, there are no reports that describe the formation of structures built of CuS and framboidal-like structures built of this mineral. Our experiments also failed to obtain CuS-framboidal-like structures.

310

## 5 Conclusions

We showed that viruses can influence the precipitation of FeS and CuS crystals. In experiments with FeS the framboid-like mineral structures have been obtained. What is more, these structures were found only in experiments conducted under static conditions without mixing, so it is possible that mixing interfered with the formation of framboid-like structures. In CuS

315 experiments, neither spherical nor framboid-like structures were noted. However, in both FeS and CuS experiments, the bacteriophages promoted the formation of finer crystallites compared to the control and influenced the agglomeration processes, as well as changes in the electrokinetic potential of mineral particles. ζ-potential measurements have also revealed that the bacteriophages probably can attract the metal ions or bind sulphide ions, depending on the presence of a lipid envelope. Hence, considering our experimental results, and the size and quantity of viruses in the natural environment, it is

320 possible that the presence of viral particles introduces one more important factor that may influence the formation of framboidal structures. Our studies are preliminary investigations, which mainly consider the shape and physicochemical properties of precipitated mineral phases with the presence of viruses. Furthermore, the process of FeS precipitation is highly limited due to the rapid oxidation of $Fe^{II}$ to stable $Fe^{III}$. However, subsequent studies might include the use of synchrotron techniques to show possible defects in the crystallographic structure caused by bacteriophages, and more importantly, to

325 discover the time-dependent processes at the beginning of the crystallisation.

**Author Contributions:** P.D. and AB designed and conducted the experiments, analysed the data, and wrote the manuscript; M.D.S. performed the XRD and SEM analyses; K.K. performed the ζ-potential measurements; M.S. and Ł.Z. contributed to writing the article.

330 **Competing interests:** The authors declare that they have no conflict of interest.

# References

335 Berner, R. A.: The synthesis of framboidal pyrite, Econ. Geol., 64, 383–384, https://doi.org/10.2113/gsecongeo.64.4.383, 1969.

Butler, I. B. and Rickard, D.: Framboidal pyrite formation via the oxidation of iron (II) monosulfide by hydrogen sulphide, Geochim. Cosmochim. Acta, 64, 2665–2672, https://doi.org/10.1016/S0016-7037(00)00387-2, 2000.

Carreira, C., Piel, T., Staal, M., Stuut, J.-B. W., Middelboe, M., and Brussaard, C. P. D.: Microscale spatial distributions of 340 microbes and viruses in intertidal photosynthetic microbial mats, SpringerPlus, 4, 239, https://doi.org/10.1186/s40064-015-0977-8, 2015.

Chen, L., Huang, L., Méndez-García, C., Kuang, J., Hua, Z., Liu, J., and Shu, W.: Microbial communities, processes and functions in acid mine drainage ecosystems, Curr. Opin. Biotechnol., 38, 150–158, https://doi.org/10.1016/j.copbio.2016.01.013, 2016.

345 Daughney, C. J., Châtellier, X., Chan, A., Kenward, P., Fortin, D., Suttle, C. A., and Fowle, D. A.: Adsorption and precipitation of iron from seawater on a marine bacteriophage (PWH3A-P1), Mar. Chem., 91, 101–115, https://doi.org/10.1016/j.marchem.2004.06.003, 2004.

Day, L. A. and Wiseman, R. L.: A Comparison of DNA Packaging in the Virions of fd, Xf, and Pf1, Cold Spring Harb. Monogr. Arch., 08, 605–625, https://doi.org/dx.doi.org/10.1101/0.605-625, 1978.

350 De Wit, R., Gautret, P., Bettarel, Y., Roques, C., Marlière, C., Ramonda, M., Nguyen Thanh, T., Tran Quang, H., and Bouvier, T.: Viruses Occur Incorporated in Biogenic High-Mg Calcite from Hypersaline Microbial Mats, PLOS ONE, 10, e0130552, https://doi.org/10.1371/journal.pone.0130552, 2015.

Donald, R. and Southam, G.: Low temperature anaerobic bacterial diagenesis of ferrous monosulfide to pyrite, Geochim. Cosmochim. Acta, 63, 2019–2023, https://doi.org/10.1016/S0016-7037(99)00140-4, 1999.

355 Farrand, M.: Framboidal sulphides precipitated synthetically, Miner. Deposita, 5, https://doi.org/10.1007/BF00201990, 1970.

Fermin, G., Mazumdar-Leighton, S., and Tennant, P.: Viruses of Prokaryotes, Protozoa, Fungi, and Chromista, in: Viruses, Elsevier, 217–244, https://doi.org/10.1016/B978-0-12-811257-1.00009-7, 2018.

Folk, R. L.: Nannobacteria and the formation of framboidal pyrite: Textural evidence, J. Earth Syst. Sci., 114, 369–374, https://doi.org/10.1007/BF02702955, 2005.

360 Fuhrman, J. A.: Marine viruses and their biogeochemical and ecological effects, Nature, 399, 541–548, https://doi.org/10.1038/21119, 1999.

Hua, X. and Buseck, P. R.: Unusual forms of magnetite in the Orgueil carbonaceous chondrite, Meteorit. Planet. Sci., 33, A215–A220, https://doi.org/10.1111/j.1945-5100.1998.tb01335.x, 1998.

Ivanovska, I. L., de Pablo, P. J., Ibarra, B., Sgalari, G., MacKintosh, F. C., Carrascosa, J. L., Schmidt, C. F., and Wuite, G. J. 365 L.: Bacteriophage capsids: Tough nanoshells with complex elastic properties, Proc. Natl. Acad. Sci., 101, 7600–7605, https://doi.org/10.1073/pnas.0308198101, 2004.

Kalatha, S. and Economou-Eliopoulos, M.: Framboidal pyrite and bacterio-morphic goethite at transitional zones between Fe–Ni-laterites and limestones: Evidence from Lokris, Greece, Ore Geol. Rev., 65, 413–425, https://doi.org/10.1016/j.oregeorev.2014.10.012, 2015.

370 Kerridge, J. F.: Some observations on the nature of magnetite in the Orgueil meteorite, Earth Planet. Sci. Lett., 9, 299–306, https://doi.org/10.1016/0012-821X(70)90122-6, 1970.

Kortenski, J. and Kostova, I.: Occurrence and morphology of pyrite in Bulgarian coals, Int. J. Coal Geol., 29, 273–290, https://doi.org/10.1016/0166-5162(95)00033-X, 1996.

Kyle, J. E., Pedersen, K., and Ferris, F. G.: Virus Mineralization at Low pH in the Rio Tinto, Spain, Geomicrobiol. J., 25, 375 338–345, https://doi.org/10.1080/01490450802402703, 2008.

Laidler, J. R. and Stedman, K. M.: Virus Silicification under Simulated Hot Spring Conditions, Astrobiology, 10, 569–576, https://doi.org/10.1089/ast.2010.0463, 2010.

Laurinavičius, S., Käkelä, R., Bamford, D. H., and Somerharju, P.: The origin of phospholipids of the enveloped bacteriophage phi6, Virology, 326, 182–190, https://doi.org/10.1016/j.virol.2004.05.021, 2004.

380 Lowenstam, H. A.: Minerals Formed by Organisms, Science, 211, 1126–1131, https://doi.org/10.1126/science.7008198, 1981.

Lowenstam, H. A. and Weiner, S.: Biomineralization Processes, in: Biomineralization Processes, Oxford University Press, https://doi.org/10.1093/oso/9780195049770.003.0005, 1989.

Mann, S.: Molecular recognition in biomineralization, Nature, 332, 119–124, https://doi.org/10.1038/332119a0, 1988.

385 Merinero, R., Lunar, R., and Somoza, L. D.-D.-R.: Nucleation, growth and oxidation of framboidal pyrite associated with hydrocarbon-derived submarine chimneys: lessons learned from the Gulf of Cadiz, Eur. J. Mineral., 21, 947–961, https://doi.org/10.1127/0935-1221/2009/0021-1956, 2009.

Muyzer, G. and Stams, A. J. M.: The ecology and biotechnology of sulphate-reducing bacteria, Nat. Rev. Microbiol., 6, 441–454, https://doi.org/10.1038/nrmicro1892, 2008.

390 Nam, K. T., Peelle, B. R., Lee, S.-W., and Belcher, A. M.: Genetically Driven Assembly of Nanorings Based on the M13 Virus, Nano Lett., 4, 23–27, https://doi.org/10.1021/nl0347536, 2004.

Nuhfer, E. B. and Pavlovic, A. S.: Association of kaolinite with pyritic framboids; discussion, J. Sediment. Res., 49, 321–323, https://doi.org/10.1306/212F772F-2B24-11D7-8648000102C1865D, 1979.

Ohfuji, H. and Akai, J.: Icosahedral domain structure of framboidal pyrite, Am. Mineral., 87, 176–180, 395 https://doi.org/10.2138/am-2002-0119, 2002.

Ohfuji, H. and Rickard, D.: Experimental syntheses of framboids—a review, Earth-Sci. Rev., 71, 147–170, https://doi.org/10.1016/j.earscirev.2005.02.001, 2005.

Orange, F., Chabin, A., Gorlas, A., Lucas-Staat, S., Geslin, C., Le Romancer, M., Prangishvili, D., Forterre, P., and Westall, F.: Experimental fossilisation of viruses from extremophilic Archaea, Biogeosciences, 8, 1465–1475, 400 https://doi.org/10.5194/bg-8-1465-2011, 2011.

Pacton, M., Wacey, D., Corinaldesi, C., Tangherlini, M., Kilburn, M. R., Gorin, G. E., Danovaro, R., and Vasconcelos, C.: Viruses as new agents of organomineralization in the geological record, Nat. Commun., 5, 4298, https://doi.org/10.1038/ncomms5298, 2014.

405 Pacton, M., Sorrel, P., Bevillard, B., Zacaï, A., Vinçon-Laugier, A., and Oberhänsli, H.: Sedimentary facies analyses from nano- to millimetre scale exploring past microbial activity in a high-altitude lake (Lake Son Kul, Central Asia), Geol. Mag., 152, 902–922, https://doi.org/10.1017/S0016756814000831, 2015.

Peng, X., Xu, H., Jones, B., Chen, S., and Zhou, H.: Silicified virus-like nanoparticles in an extreme thermal environment: implications for the preservation of viruses in the geological record, Geobiology, n/a-n/a, https://doi.org/10.1111/gbi.12052, 2013.

410 Pennafirme, S., Pereira, D. C., Pedrosa, L. G. M., Machado, A. S., Silva, G. O. A., Keim, C. N., Lima, I., Lopes, R. T., Paixão, I. C. N. P., and Crapez, M. A. C.: Characterization of microbial mats and halophilic virus-like particles in a eutrophic hypersaline lagoon (Vermelha Lagoon, RJ, Brazil), Reg. Stud. Mar. Sci., 31, 100769, https://doi.org/10.1016/j.rsma.2019.100769, 2019.

Perri, E., Tucker, M. E., Słowakiewicz, M., Whitaker, F., Bowen, L., and Perrotta, I. D.: Carbonate and silicate
415 biomineralization in a hypersaline microbial mat (Mesaieed sabkha, Qatar): Roles of bacteria, extracellular polymeric substances and viruses, Sedimentology, 65, 1213–1245, https://doi.org/10.1111/sed.12419, 2018.

Perri, E., Słowakiewicz, M., Perrotta, I. D., and Tucker, M. E.: Biomineralization processes in modern calcareous tufa: Possible roles of viruses, vesicles and extracellular polymeric substances (Corvino Valley – Southern Italy), Sedimentology, 69, 399–422, https://doi.org/10.1111/sed.12932, 2022.

420 Popa, R., Kinkle, B. K., and Badescu, A.: Pyrite Framboids as Biomarkers for Iron-Sulfur Systems, Geomicrobiol. J., 21, 193–206, https://doi.org/10.1080/01490450490275497, 2004.

Scott, R. J., Meffre, S., Woodhead, J., Gilbert, S. E., Berry, R. F., and Emsbo, P.: Development of Framboidal Pyrite During Diagenesis, Low-Grade Regional Metamorphism, and Hydrothermal Alteration, Econ. Geol., 104, 1143–1168, https://doi.org/10.2113/gsecongeo.104.8.1143, 2009.

425 Slocik, J. M., Naik, R. R., Stone, M. O., and Wright, D. W.: Viral templates for gold nanoparticle synthesis, J. Mater. Chem., 15, 749, https://doi.org/10.1039/b413074j, 2005.

Słowakiewicz, M., Borkowski, A., Syczewski, M. D., Perrota, I. D., Owczarek, F., Sikora, A., Detman, A., Perri, E., and Tucker, M. E.: Newly-discovered interactions between bacteriophages and the process of calcium carbonate precipitation, Geochim. Cosmochim. Acta, 292, 482–498, https://doi.org/10.1016/j.gca.2020.10.012, 2021.

430 Steward, G., Smith, D., and Azam, F.: Abundance and production of bacteria and viruses in the Bering and Chukchi Seas, Mar. Ecol. Prog. Ser., 131, 287–300, https://doi.org/10.3354/meps131287, 1996.

Taylor, G. R.: A mechanism for framboid formation as illustrated by a volcanic exhalative sediment, Miner. Deposita, 17, https://doi.org/10.1007/BF00206374, 1982.

Vidaver, A. K., Koski, R. K., and Etfen, J. L. V.: Bacteriophage θ6: a Lipid-Containing Virus of Pseudomonas phaseolicolal,
435 J. Virol., 11, 799–805, https://doi.org/10.1128/JVI.11.5.799-805.1973, 1973.

Wang, Q. and Morse, J. W.: Pyrite formation under conditions approximating those in anoxic sediments I. Pathway and morphology, Mar. Chem., 52, 99–121, https://doi.org/10.1016/0304-4203(95)00082-8, 1996.

White, T. S., Morrison, J. L., and Kump, L. R.: Formation of Iron Sulfides in Modern Salt Marsh Sediments (Wallops Island, Virginia), in: Geochemistry of Sulfur in Fossil Fuels, vol. 429, American Chemical Society, 204–217, https://doi.org/10.1021/bk-1990-0429.ch011, 1990.

440

Wiese, R. G. and Fyfe, W. S.: Occurrences of iron sulfides in Ohio coals, Int. J. Coal Geol., 6, 251–276, https://doi.org/10.1016/0166-5162(86)90004-2, 1986.

Wilkin, R., Arthur, M., and Dean, W.: History of water-column anoxia in the Black Sea indicated by pyrite framboid size distributions, Earth Planet. Sci. Lett., 148, 517–525, https://doi.org/10.1016/S0012-821X(97)00053-8, 1997.

445     Wilkin, R. T. and Barnes, H. L.: Formation processes of framboidal pyrite, Geochim. Cosmochim. Acta, 61, 323–339, https://doi.org/10.1016/S0016-7037(96)00320-1, 1997.

Wilkin, R. T., Barnes, H. L., and Brantley, S. L.: The size distribution of framboidal pyrite in modern sediments: An indicator of redox conditions, Geochim. Cosmochim. Acta, 60, 3897–3912, https://doi.org/10.1016/0016-7037(96)00209-8, 1996.

450     Wittebole, X., De Roock, S., and Opal, S. M.: A historical overview of bacteriophage therapy as an alternative to antibiotics for the treatment of bacterial pathogens, Virulence, 5, 226–235, https://doi.org/10.4161/viru.25991, 2014.

Wolthers, M.: Geochemistry and environmental mineralogy of the iron-sulphur-arsenic system: = Geochemie en milieumineralogie van het ijzer-zwavel-arseen systeem, Univ, Utrecht, 185 pp., 2003.

Wolthers, M., Butler, I. B., Rickard, D., and Mason, P. R. D.: Arsenic Uptake by Pyrite at Ambient Environmental
455     Conditions: A Continuous-Flow Experiment, in: Advances in Arsenic Research, vol. 915, American Chemical Society, 60–76, https://doi.org/10.1021/bk-2005-0915.ch005, 2005.
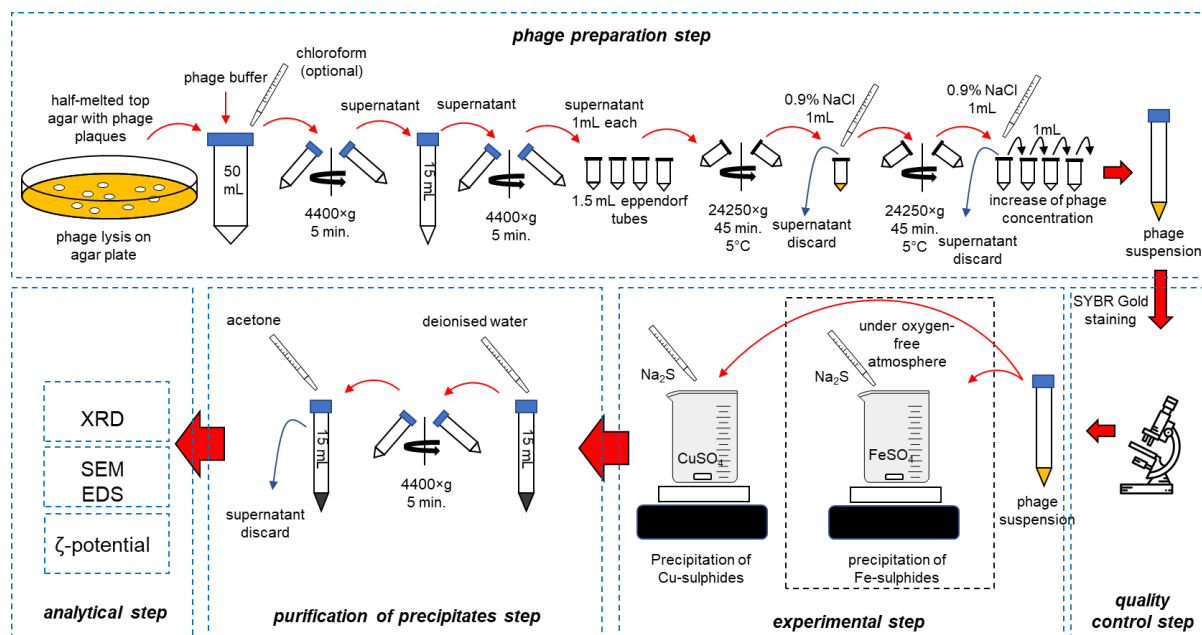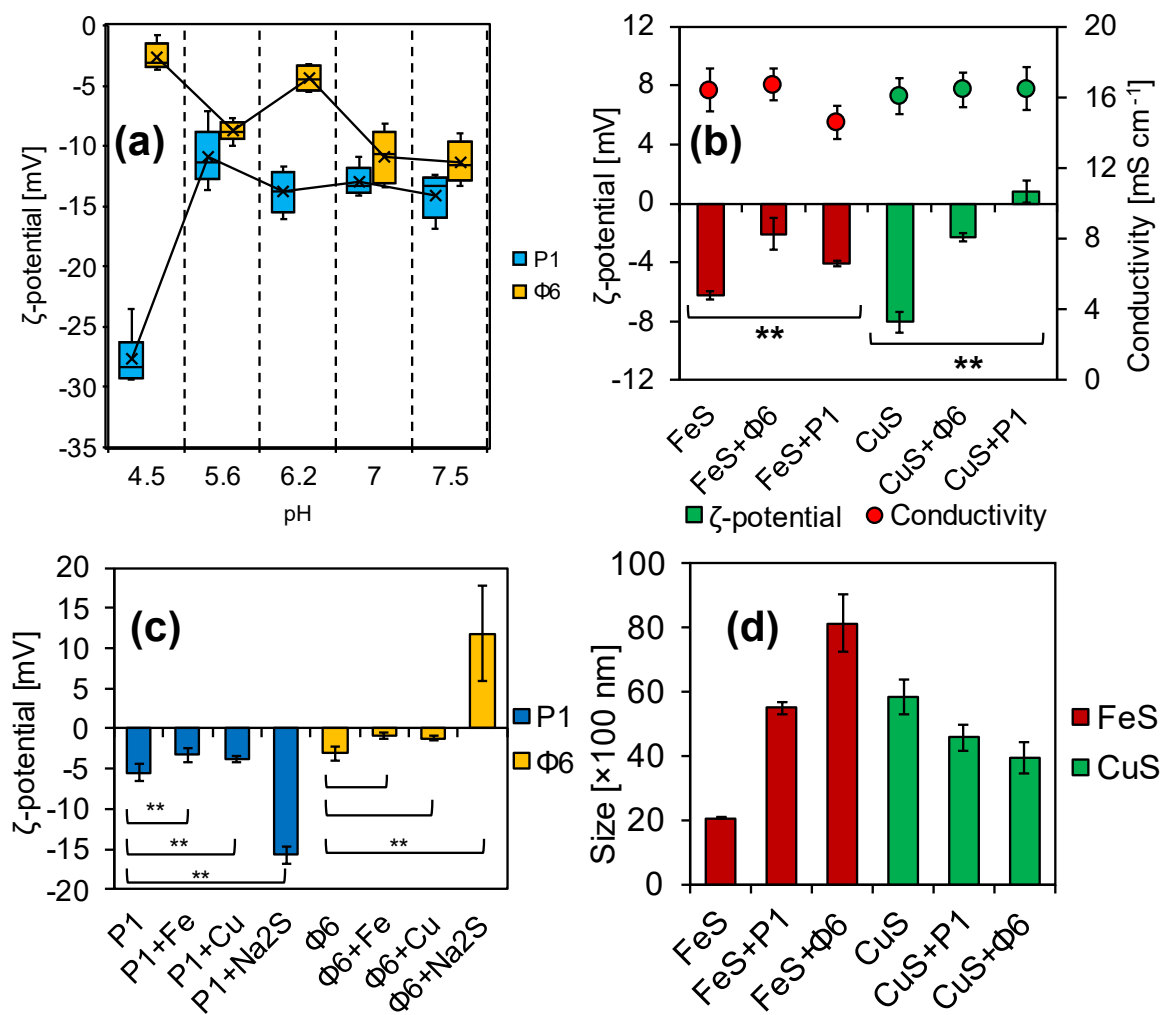
460 **Figure 1. The scheme of experiments.**
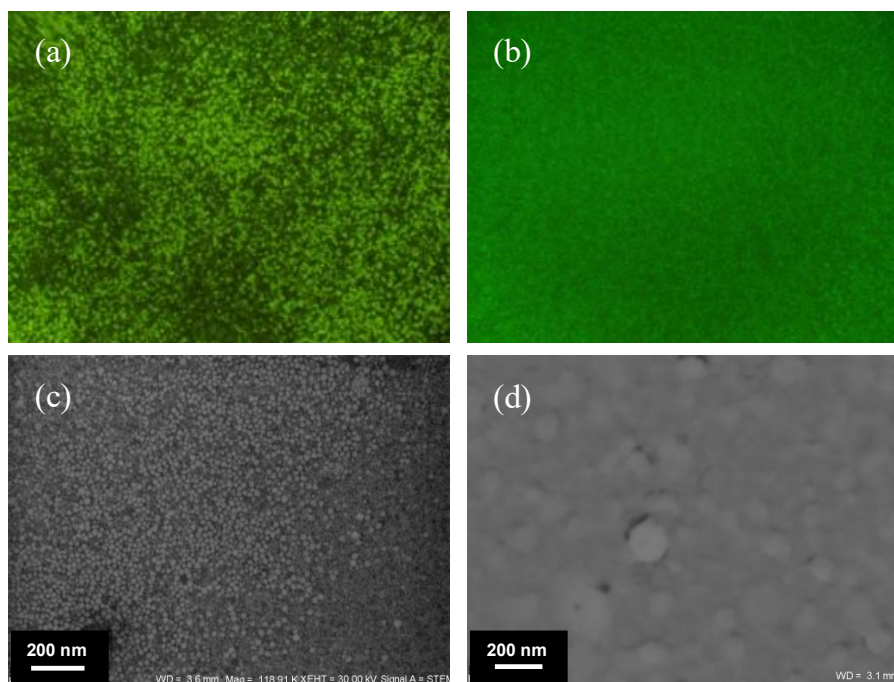
465 **Figure 2. Purified bacteriophages stained with SybrGold® (magnification 400×), (a) Enterobacteria phage P1, (b) Pseudomonas phage Φ6; and SEM images, (c) Enterobacteria phage P1 stained with uranyl nitrate, (d) Pseudomonas phage Φ6 without staining.**

**Figure 3. Electrochemical properties of (a) viruses, (b) FeS and CuS precipitates with/without presence of viruses; (c) attraction of ions by bacteriophages; (d) Z-average size distribution of FeS and CuS. ** indicates statistical significance.**
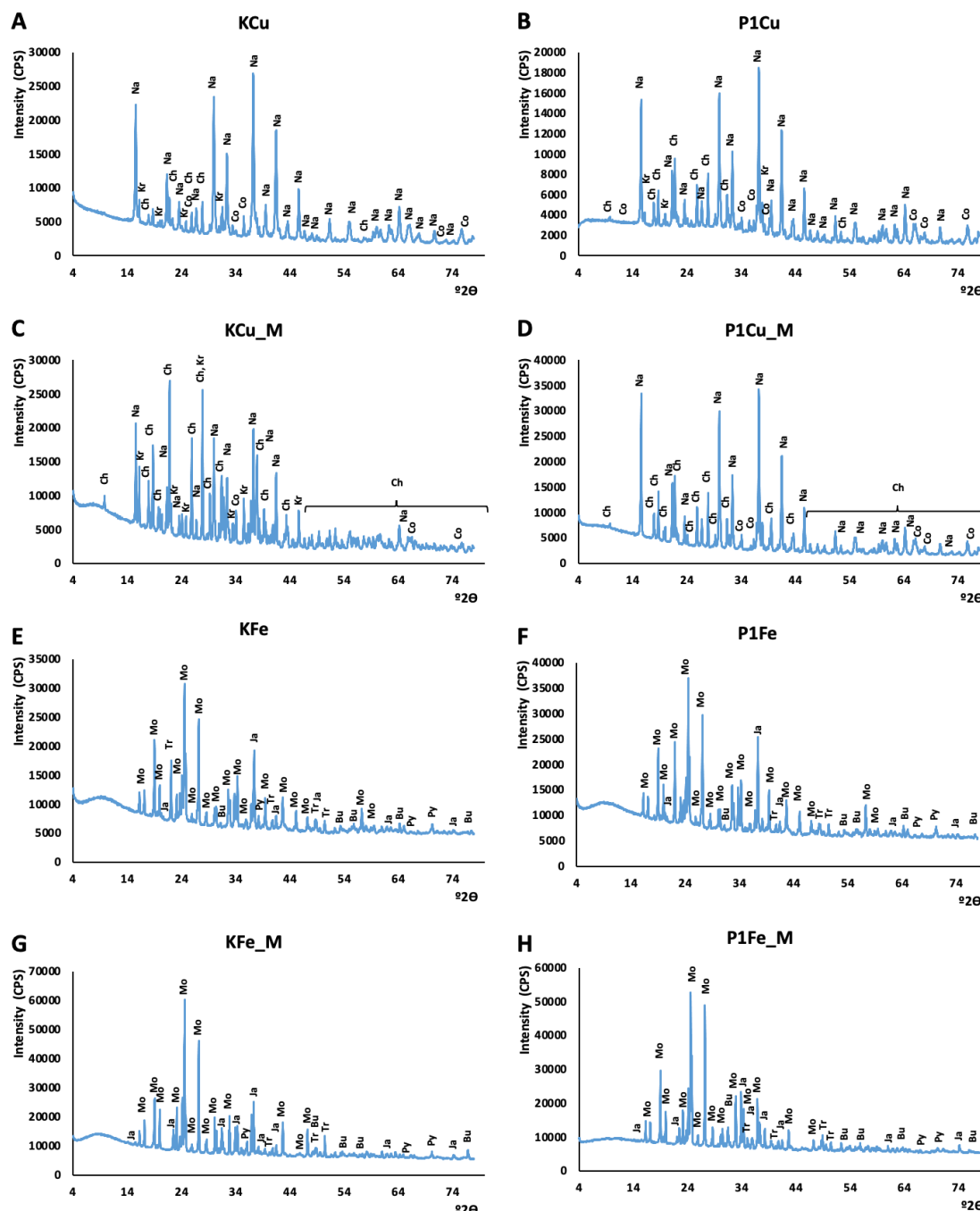
**Figure 4. XRD patterns of synthesised phases. The copper sulphide experiment without mixing: control experiment (A), P1 phage experiment (B). The copper sulphide experiment with mixing: control experiment (C), P1 phage experiment (D). The iron sulphide experiment without mixing: control experiment (E), P1 phage experiment (F). The iron sulphide experiment with mixing: control experiment (G), P1 phage experiment (H). Bu – butlerite, Ch – chalkantite, Kr – kröhnkite, Na – natrochalcite, Co – covellite, Tr – troillite, Py – pyrite, Mo – mohrite.**
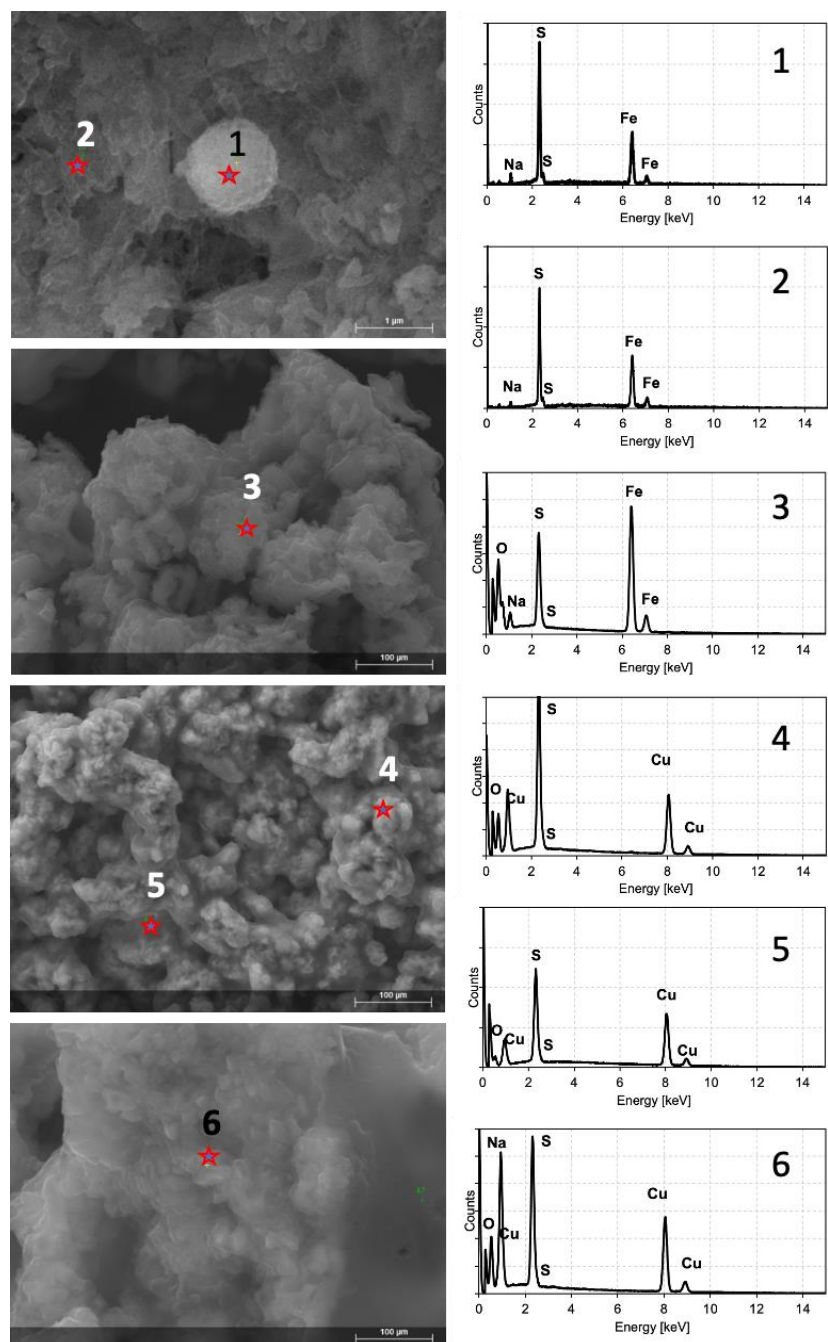
**Figure 5. SEM images and EDS spectra characterizing the observed mineral phases after experiments. Spectra 1 and 2 indicate FeS precipitates. Spectrum 3 probably indicates sulphates due to the strong oxygen signal in relation to sulphur. Spectra 4 and 5 indicate CuS phases. Spectrum 6 indicates possible impurities due to the presence of sodium (strong signal in relation to sulphur).**
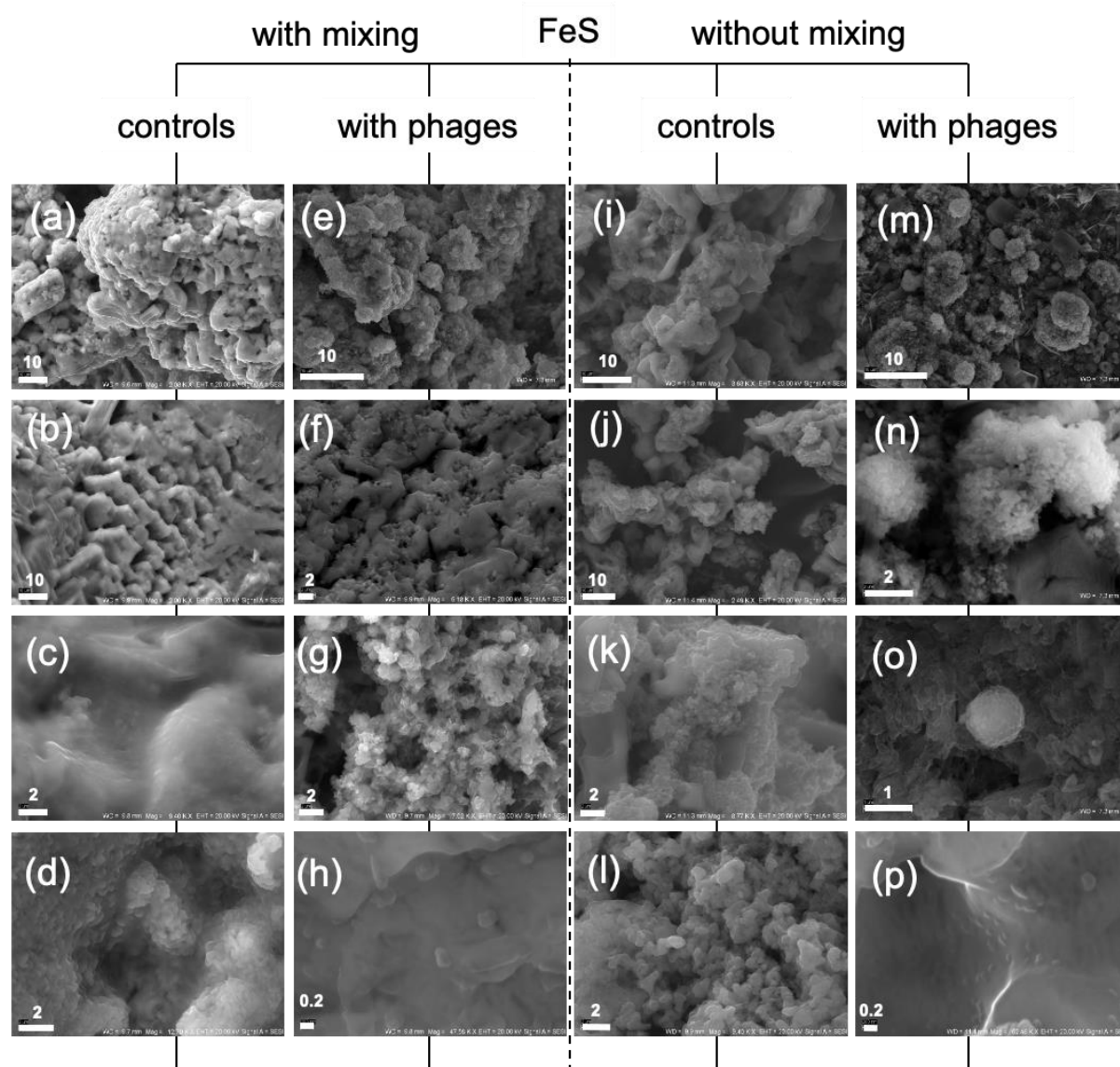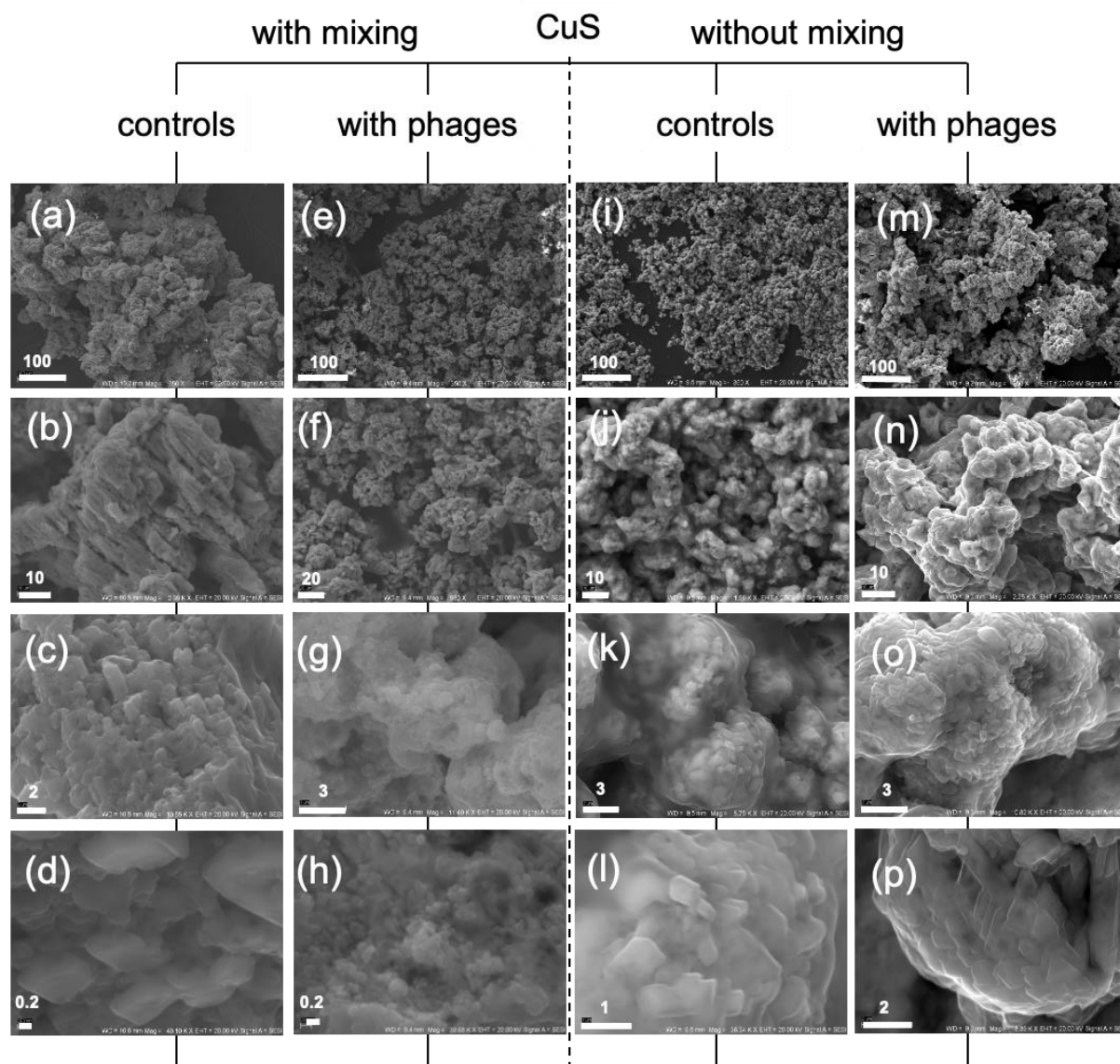
**Figure 6. FeS precipitates under SEM after experiments with P1 bacteriophages. (a-d) – mineral phases precipitated without bacteriophages under mixing conditions; (e-h) – mineral structures obtained in experiment with bacteriophages under mixing conditions; (i-l) – mineral phases precipitated without bacteriophages under static (without mixing) conditions; (m-p) – mineral phases precipitated with bacteriophages under static conditions; (m) and (o) show spherical structures resembling protoframboids. Bar indicates scale in μm.**
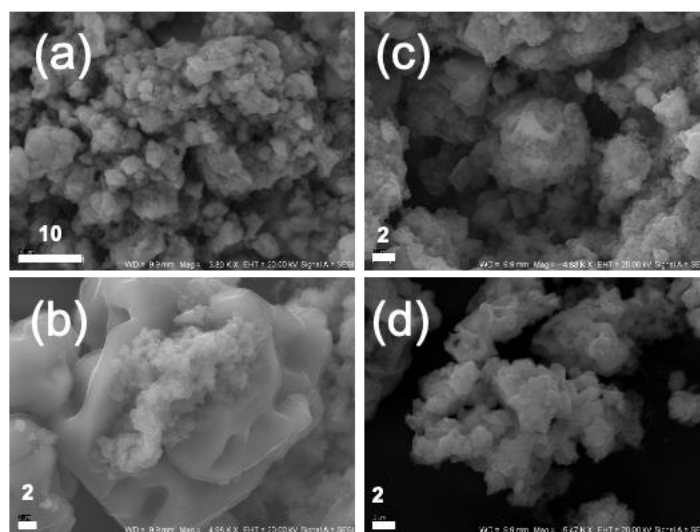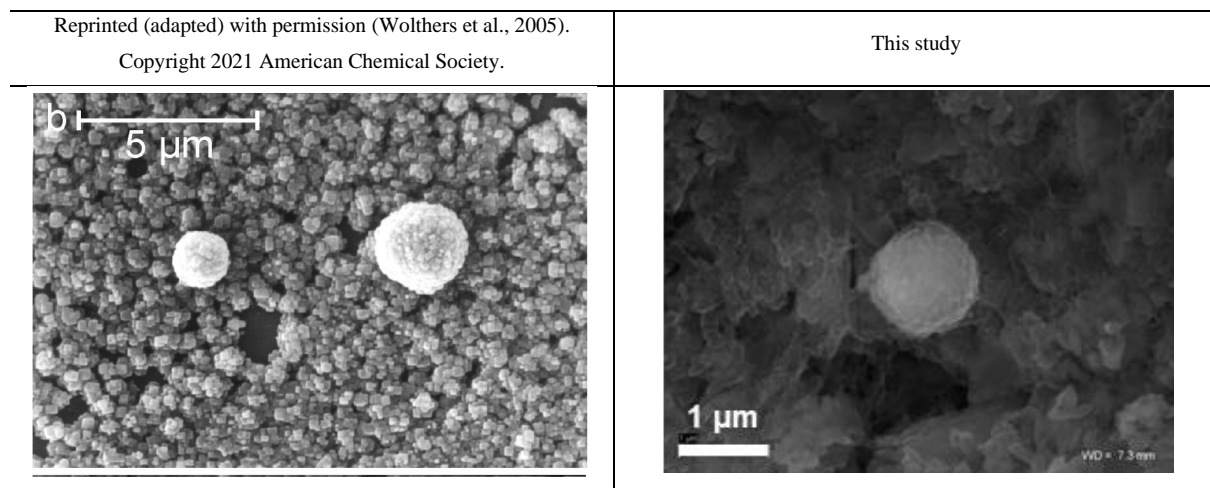
**Figure 7. FeS precipitates under SEM after experiments with Φ6 phage. (a-b) – mineral phases obtained in experiment under mixing conditions; (c-d) – mineral phases precipitated under static (without mixing) conditions. The bar indicates scale in μm.**

**Figure 8. CuS mineral phases under SEM after experiments with the P1 phage. (a-d) – mineral structures precipitated without bacteriophages under mixing conditions; (e-h) – mineral phases obtained in experiment with bacteriophages under mixing conditions; (i-l) – mineral phases precipitated without bacteriophages under static (without mixing) conditions; (m-p) – mineral phases precipitated with bacteriophages under static conditions. Bar indicates scale in µm.**

495

500

| Reprinted (adapted) with permission (Wolthers et al., 2005). Copyright 2021 American Chemical Society. | This study |
|---|---|



**Figure 9. The framboidal structures obtained by Wolthers (Wolthers et al., 2005) and obtained during our experiments. Note nearly identical framboid shapes in both cases but under different experimental conditions.**
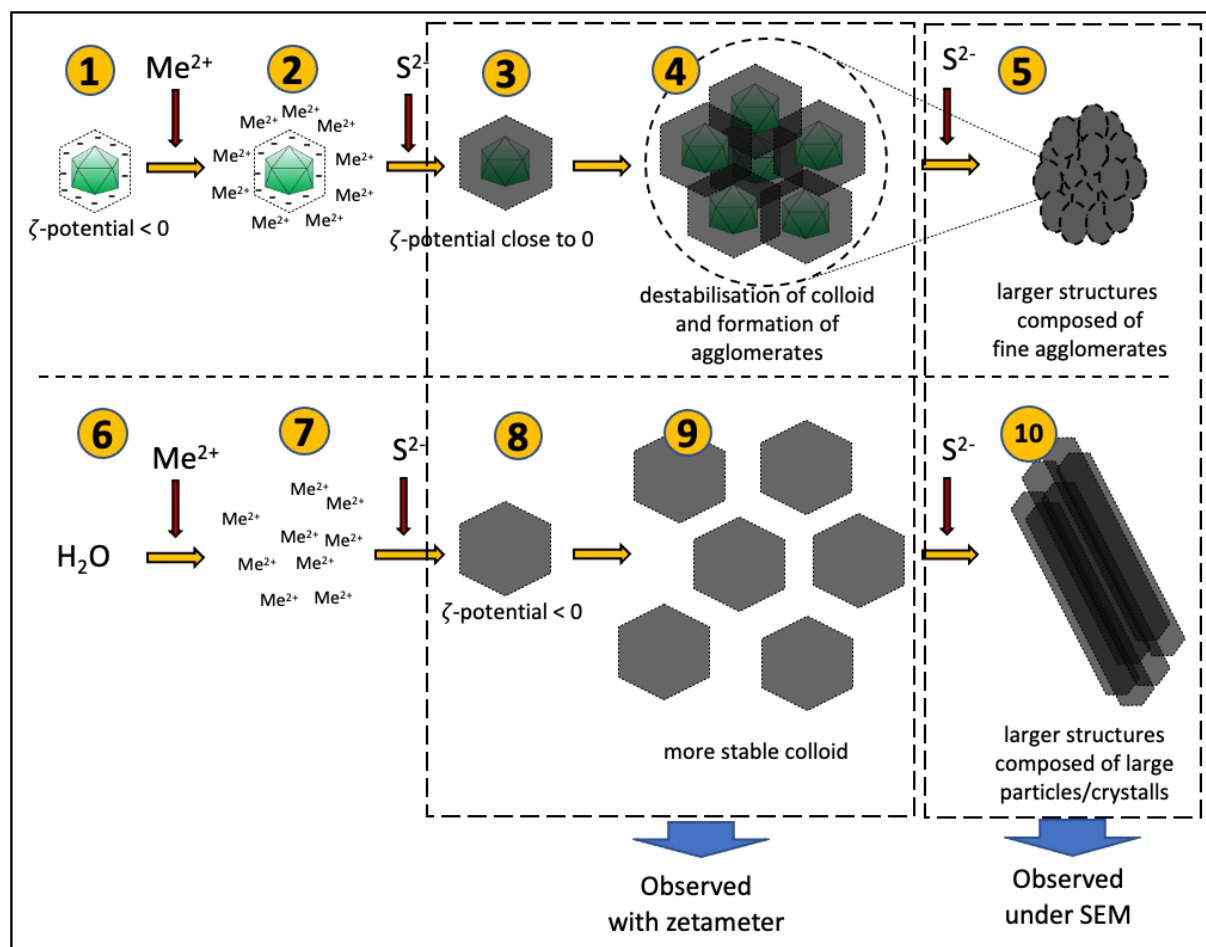
**Figure 10. Hypothetical processes leading to the observed phenomena. Negatively charged bacteriophages capsids attract metal ions (1-2). When sulphide ions in small amounts are added, sulphides will precipitate on capsids (3). Due to surface charge close to zero, the colloid undergoes destabilization and agglomerates can be formed (4). Addition of more sulphides can promote creation of more such agglomerates which can lead to the larger structure (composed of small agglomerates) (5). The addition of small portion of sulphides in experiment without bacteriophages (6-8) can lead to the formation of more stable colloid due to lower ζ-potential (9). However, the addition of more sulphide ions causes further growth of crystals and formation of larger structures composed of large particles or crystals.**